Hossein Derakhshan, Yasuto Nakamura, Jason M. Ingham & Michael C. Griffith
Simulation of shake table tests on out-of-plane masonry buildings. Part (I): displacement-based approach using simple failure mechanisms
International Journal of Architectural Heritage: conservation, analysis, and restoration, 2017; 11(1):72-78

International Journal of Architectural Heritage
Conservation, Analysis, and Restoration

ISSN: 1558-3058 (Print) 1558-3066 (Online) Journal homepage: http://www.tandfonline.com/loi/uarc20

SIMULATION OF SHAKE TABLE TESTS ON OUT-OF-PLANE MASONRY BUILDINGS. PART (I): DISPLACEMENT-BASED APPROACH USING SIMPLE FAILURE MECHANISMS

Hossein Derakhshan, Yasuto Nakamura, Jason M. Ingham & Michael C. Griffith

To cite this article: Hossein Derakhshan, Yasuto Nakamura, Jason M. Ingham & Michael C. Griffith (2016): SIMULATION OF SHAKE TABLE TESTS ON OUT-OF-PLANE MASONRY BUILDINGS. PART (I): DISPLACEMENT-BASED APPROACH USING SIMPLE FAILURE MECHANISMS, International Journal of Architectural Heritage, DOI: 10.1080/15583058.2016.1237590

To link to this article: http://dx.doi.org/10.1080/15583058.2016.1237590

Accepted author version posted online: 22 Sep 2016.

Simulation of shake table tests on out-of-plane masonry buildings. Part (I): Displacement-based approach using simple failure mechanisms

Hossein Derakhshan[1], Yasuto Nakamura[2], Jason M. Ingham[3], and Michael C. Griffith[4]

Abstract

A displacement-based (DB) assessment procedure was used to predict the results of shake table testing of two unreinforced masonry buildings, one made of clay bricks and the other of stone masonry. The simple buildings were subject to an acceleration history, with the maximum acceleration incrementally increased until a collapse mechanism formed. Using the test data, the accuracy and limitations of a displacement-based procedure to predict the maximum building displacements are studied. In particular, the displacement demand was calculated using the displacement response spectrum corresponding to the actual shake table earthquake motion that caused wall collapse (or near collapse). This approach was found to give displacements in reasonable agreement with the wall's displacement capacity.

[1] Research Associate, University of Adelaide
[2] PhD student, University of Adelaide
[3] Professor, University of Auckland
[4] Professor, University of Adelaide

Introduction

One clay brick and one stone unreinforced building having nominally identical characteristics other than their wall morphology were tested on the shake table at the National Laboratory for Civil Engineering, Portugal, and the collapse mechanism and the corresponding acceleration data were recorded, see (Candeias et al. 2016). The failure mechanism for both buildings was in the form of partial out-of-plane collapse of the buildings' façades. The study reported herein attempts to reproduce the peak ground acceleration (PGA) associated with the collapse of the buildings using the displacement-based assessment method presented in (Griffith et al. 2003).

To assess the seismic response of any building it is imperative to identify failure mechanism(s). During the prediction stage of this study, i.e. prior to testing, conceptually possible failure mechanisms for the two simple buildings were identified based on engineering judgement as one of: (1) out-of-plane failure of the façade with separation from corners, (2) out-of-plane failure with partial flange rocking, or (3) partial out-of-plane failure without flange damage. To determine the governing failure mechanism for each building, calculations were first conducted using methodology developed by (Vaculik 2012) (an alternative method is to use the designers formula available in Section 7 of Australian standard for Masonry Structures, AS 3700, (Standards Australia, 2011) to estimate the two-way out-of-plane strength of the façade considering the restraints along three of the wall edges and the free top edge. As part of the method, the adequacy of the strength of the flanges to promote development of the full strength in the two-way spanning façade was then checked.

Failure mechanisms; predictions vs real

Clay brick masonry building:

Two potential failure mechanisms were investigated for the brick masonry building, one being based on dry stack masonry (DSM) construction (Restrepo Vélez et al. 2014; Vaculik et al. 2014), and the other based on the two-way bending strength of URM walls. The DSM-based mechanism (not reported herein) did not closely match the actual failure, highlighting the important influence of tensile bond strength on the collapse mechanism and associated strength.

The mechanism (M1 in Figure 1a) based on the two-way bending strength calculation of the façade and the orthogonal flanges was close to the observed damage behaviour and is reviewed here in detail.

In the prediction stage of the study, the two-way bending capacity (Vaculik 2012) of the out-of-plane loaded façade was calculated assuming support along three edges (top edge being free) and the opening. The factor as defined in (Vaculik 2012) that relates to rotational fixity along the vertical edges was assumed to be 0.5. Assuming that the façade developed its full out-of-plane capacity, the resulting tensile reaction force applied to the in-plane loaded piers was calculated and compared with the pier tensile strength. It was found that the flange wall with an opening could not provide the reaction support required for the façade to develop its full out-of-plane capacity. Consequently it was envisaged that the flange was a part of the rocking assemblage (Mechanism M1 in Figure 1a).

Inspection of the videos of the shake table tests revealed that the predicted failure mechanism for the brick building was accurate, but that a secondary mechanism that resulted in the wall collapse was formed after initiation of the first mechanism. The second mechanism was the

rocking of the top wall segment consisting of the gable and a small section of the wall below eaves level (Mechanism M2 in Figure 1b). The calculations presented in the following sections are therefore based on this latter mechanism.

Stone masonry building:

A similar methodology was used to determine the failure mechanism of the stone masonry building. It was found that the in-plane loaded piers in the stone masonry building were sufficiently strong to allow the façade to develop its full out-of-plane two-way bending strength. It was therefore concluded that the failure mechanism would be in the form of out-of-plane cracking of the façade with separation from the corners. Investigation of video recordings of the shake table tests suggested that the predicted mechanism was mostly correct as the mechanism did include part of the in-plane wall while not including all of the building façade, as sketched in Figure 2. This observation suggests that the pre-test calculations overestimated the in-plane shear capacity of the stone pier with an opening, possibly due to the employed methods being based on research conducted on brick masonry.

Effective SDOF system properties

Due to the shape of the rocking segments of the building facades being irregular, the assessment method presented in (Doherty et al. 2002) could not be directly used, although the same principles were used to obtain the mass and stiffness properties of the equivalent single-degree-of-freedom (SDOF) system.

The mode shape and mass distribution diagrams shown in Figure 3 and Figure 4 were used to calculate the effective mass and displacement values for the identified mechanisms (M2, i.e. Figure 1b, for the brick building, and Figure 2 for the stone building). These effective

quantities can be calculated using Eqs. 1 and 2, and Columns 2 and 3 of Table 1 summarise the calculated values.

$$M_{eff} = \frac{[\int m.\varphi dz]^2}{\int m.\varphi^2 dz} \quad \text{Eq. 1}$$

$$\Delta_{eff} = \frac{\int m.\Delta^2(z)dz}{\int m.\Delta(z)dz} \quad \text{Eq. 2}$$

with m and φ being the vertical mass distributions and mode shapes defined in Figure 3 and Figure 4, respectively, for the brick and the stone buildings. Δ(z) is defined as the lateral displacement at any given height:

$$\Delta(z) = \varphi.\Delta_t \quad \text{Eq. 3}$$

Δ_t in Eq. 3 is the control displacement defined in the following paragraph.

The free-body diagram of the rocking segments of the building facades, as shown in Figure 5 and Figure 6, are analysed to establish bilinear rigid force-displacement curves, on which basis the equivalent SDOF system properties can be calculated. The displacement at the top of the gable, $\Delta_{t,}$ was assumed as the control displacement and the instability displacement, $\Delta_{t,ins}$ and the uniformly distributed horizontal acceleration at rocking threshold, $a_{ins,}$ were calculated as summarised in Columns 4 and 5 of Table 1. To obtain $\Delta_{t,ins}$ and a_{ins}, an equation representing the sum of bending moments about the rocking pivot (point "A" in Figure 5 and Figure 6) is first written. The instability displacement and acceleration at rocking threshold are then calculated by equating, respectively, a and Δ_t to zero.

The trilinear curves can be established using coefficients suggested by Derakhshan et al. 2014, with $\Delta_{1,eff} = 0.04\Delta_{ins,eff}$, $\Delta_{2,eff} = 0.25\Delta_{ins,eff}$, and the idealised force, $F_{i,eff} = 0.75\ F_{0,eff}$. Figure 7 and Figure 8 show the trilinear curves calculated for the rocking segments of the

buildings. It should be noted that both the displacement and the force ordinates of the graphs in Figure 7 and Figure 8 are effective quantities, and therefore the displacement values are based on Column 3 (rather than 4) of Table 1. Similarly, the force values are based on the calculated acceleration (Column 5) and the effective mass (Column 2). The secant stiffness, $K_{2,eff}$, can therefore be calculated as listed in Column 6 of Table 1.

Using the calculated effective stiffness, $K_{2,eff}$, and the effective mass, the effective period, T_2, can be calculated as listed in Column 7 of Table 1.

Estimation of collapse

Elastic displacement spectra were derived directly from the accelerations measured on the shake table, and the secant periods (T_2) calculated on the basis of the experimentally observed crack patterns as detailed in Table 1 are used to estimate the maximum displacement response.

The maximum displacements of the effective SDOF systems representative of the two buildings were calculated using the periods, T_2, listed in Table 1, and 5% damped response spectra for various levels of shaking as detailed in Table 2 and plotted in Figure 9. It is noted that the calculated displacements using T_2 are effective displacements and are therefore translated, as detailed in Table 2, to displacements at top, Δ_t, by dividing by the relevant factors from Table 1, i.e. 0.560 for brick and 0.505 for stone building. These calculated displacements have been compared to the corresponding measured displacements from LVDTs. Consistent with Griffith et al. (2003) findings, T_2 is a good measure of the equivalent

linear system period if the wall maximum displacement exceeds half the displacement capacity.

For the cases that the wall maximum displacement remains insignificant relative to the wall displacement capacity, either because the wall is not cracked, e.g. tests 1-5 for brick building and 1-3 for the stone building, or the rocking amplitude is insignificant relative to the wall displacement capacity, e.g. tests 6-7 for brick building and 4-5 for the stone building, the assumption of T_2 as the linear equivalent system is overly conservative. In practice, the rocking amplitude of the wall is not known before assessment even if cracking has been established. This problem renders the displacement-based procedure to be always conservative. Conducting a two-tier assessment consisting of an initial strength capacity check to establish cracking and, where necessary, a subsequent displacement-based assessment reduces the degree of conservatism.

Once the full collapse mechanisms formed in the final tests, the displacement-based analyses give good predictions of the experimental results for both buildings. The collapse of the brick building was correctly predicted, for the range of damping ratios between 2% and 10%, considered to encompass the likely range of damping for rocking walls (Figure 10, note that the values are shown in the transformed coordinates corresponding to the equivalent single-degree-of-freedom definition of the mechanism). Perhaps more significantly, the non-collapse of the stone wall is also correctly predicted (Figure 11). Furthermore, supposing a 5% viscous damping ratio, the peak displacement demand of the stone wall is estimated to be 0.208 m at the top, which is in a good agreement with the measured peak displacement of 0.219 m.

From the preceding discussion, the displacement-based analysis using the secant stiffness appears to be a viable simplified procedure in estimating the peak displacement demands of walls undergoing rocking. However, the procedure can result in large overestimations when the wall does not undergo rocking, for example, if it remains almost elastic. In practical applications, therefore, it appears prudent to ensure that the bending strength of the wall is at least exceeded by the imposed inertial force before carrying out the collapse check using the substitute-structure approach.

Conclusions

The accuracy of a displacement-based method has been evaluated based on the observed cracking pattern of the buildings. It has been found that subject to correct prediction of the failure mechanism, first principles can be used to determine the substitute-structure dynamic properties and the method appears to be a viable simplified procedure in estimating the peak displacement demands near collapse. The procedure can result in large overestimations when the wall does not undergo rocking, i.e. in small displacement range relative to instability displacement. In practical applications, therefore, it appears prudent to ensure that the bending strength of the wall is at least exceeded by the imposed inertial force before carrying out the collapse check using the substitute-structure approach.

References

Candeias, P.X, Campos Costa, A., Mendes, N., Costa, A.A., and Lourenço, P.B. 2016. Experimental assessment of the out of plane performance of masonry buildings through shake table tests. *International Journal of Architectural Heritage*, This issue.

Derakhshan, H., D. Y. Dizhur, M. C. Griffith, and J. M. Ingham. 2014. Seismic assessment of out-of-plane loaded unreinforced masonry walls in multi-storey buildings. *Bulletin of the New Zealand Society for Earthquake Engineering* 47 (2):119-138.

Doherty, K., M. C. Griffith, N. Lam, and J. Wilson. 2002. Displacement-based seismic analysis for out-of-plane bending of unreinforced masonry walls. *Earthquake Engineering and Structural Dynamics* 31 (4):833-850.

Griffith, M. C., G. Magenes, G. Melis, and L. Picchi. 2003. Evaluation of out-of-plane stability of unreinforced masonry walls subjected to seismic excitation. *Journal of Earthquake Engineering* 7 (SPEC. 1):141-169.

Restrepo Vélez, L. F., G. Magenes, and M. C. Griffith. 2014. Dry stone masonry walls in bending-Part I: Static tests. *International Journal of Architectural Heritage* 8 (1):1-28.

Standards Australia (2011), Masonry Structures (AS 3700 – 2011), SA, Homebush, NSW.

Vaculik, J., M. C. Griffith, and G. Magenes. 2014. Dry stone masonry walls in bending-Part II: Analysis. *International Journal of Architectural Heritage* 8 (1):29-48

Vaculik, J. 2012. Unreinforced masonry walls subjected to out-of-plane seismic actions. Ph.D., School of Civil, Environmental, and Mining Engineering, University of Adelaide, PhD Thesis, Adelaide.

Figure 1: Failure mechanisms of the brick building

a) M1 b) M2

Figure 2: Failure mechanism of the stone building

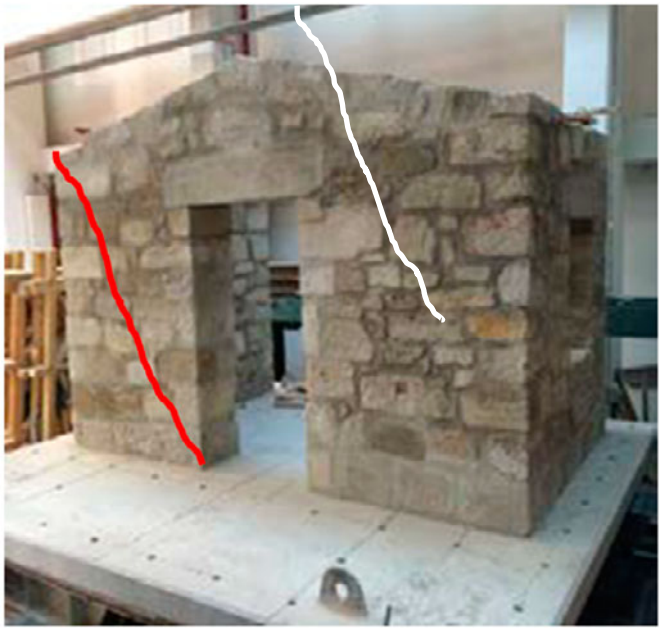

Figure 3: The failure mechanism and SDOF idealisation of the brick façade; circled numbers indicate areas referred to in Figure 5 (diagrams not to scale)

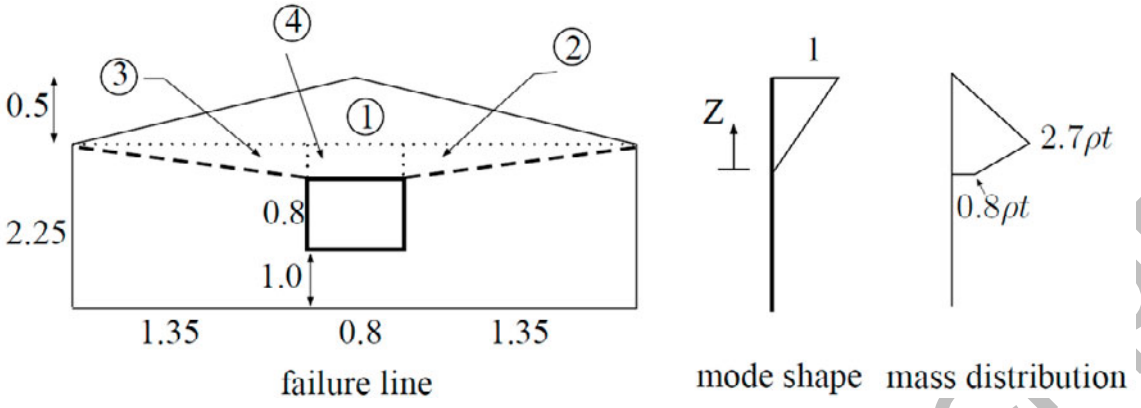

Figure 4: Façade of the stone building; circled numbers indicate areas referred to in Figure 6 (diagrams not to scale)

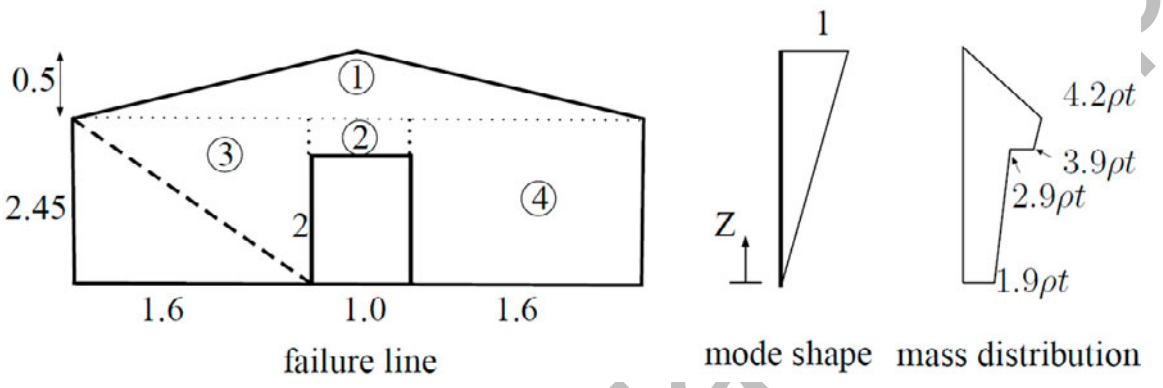

Figure 5: Free-body diagram of the rocking gable of the brick building; "a" is a uniform horizontal acceleration, dimensions are in m units, and point A corresponds to z=0 in Figure 3

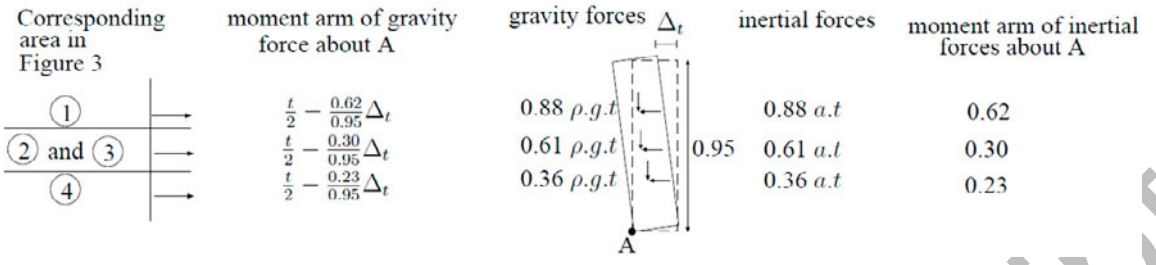

Figure 6: Free-body diagram of the rocking façade of the stone building; "a" is a uniform horizontal acceleration, dimensions are in m units, and point A corresponds to z=0 in Figure 4

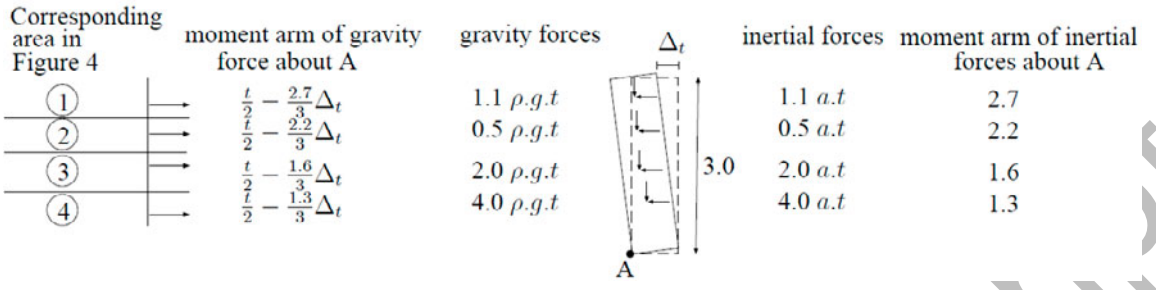

Figure 7: The trilinear model of the representative effective SDOF of brick gable

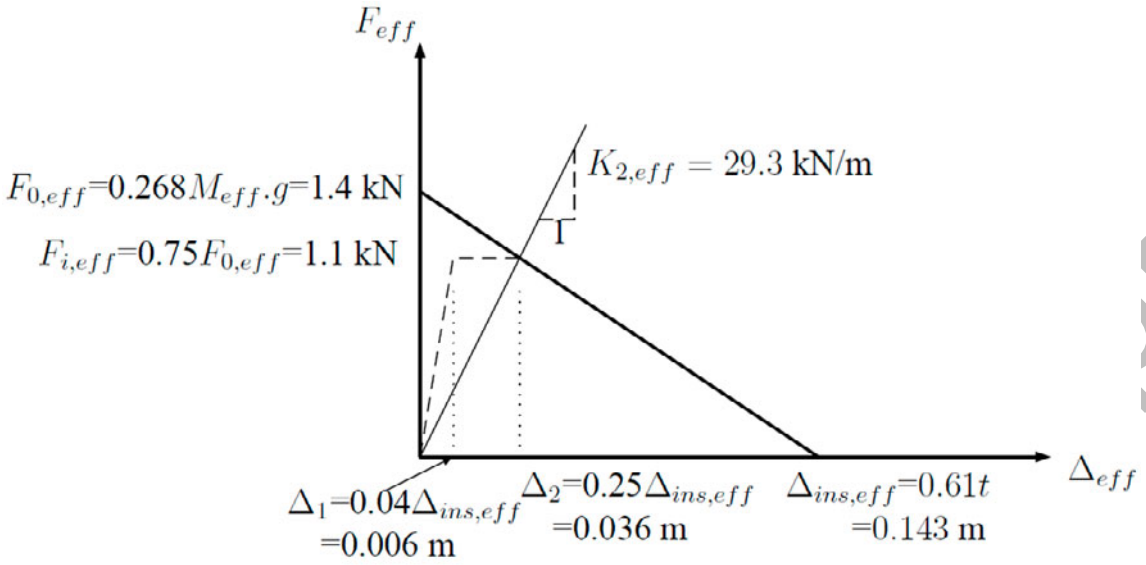

Figure 8: The trilinear model of the representative effective SDOF of stone façade

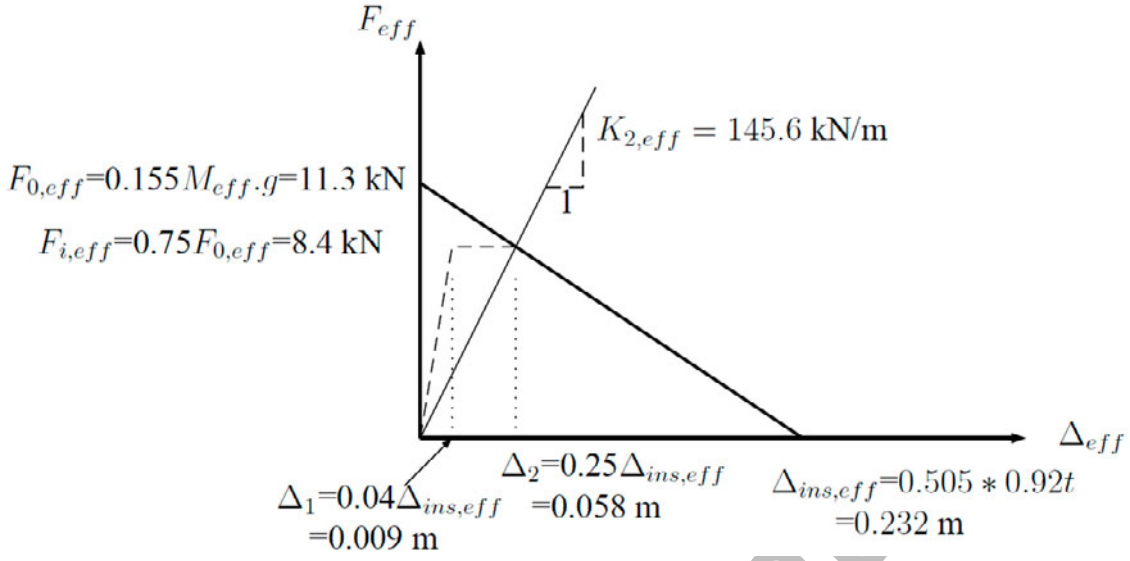

Figure 9: Displacement prediction by the displacement-based method

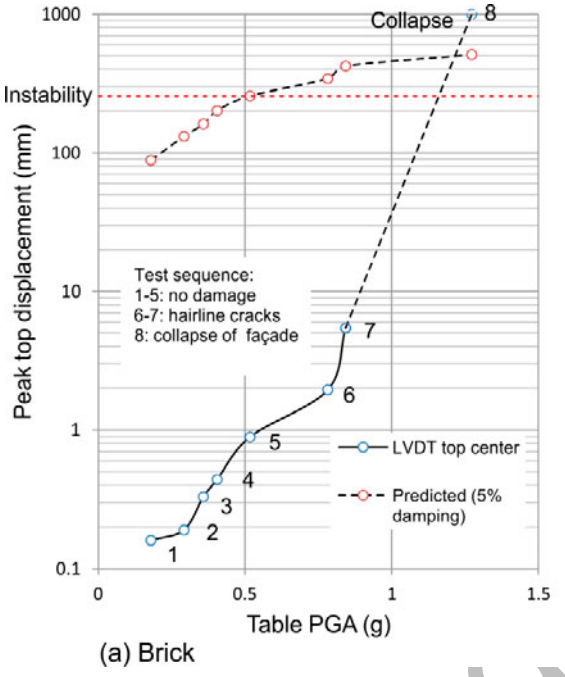

(a) Brick

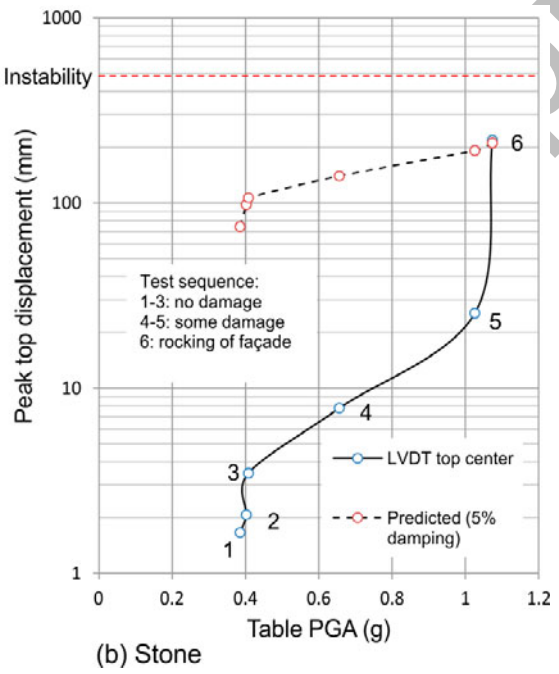

(b) Stone

Figure 10: Displacement assessment of the brick building façade under the largest excitation

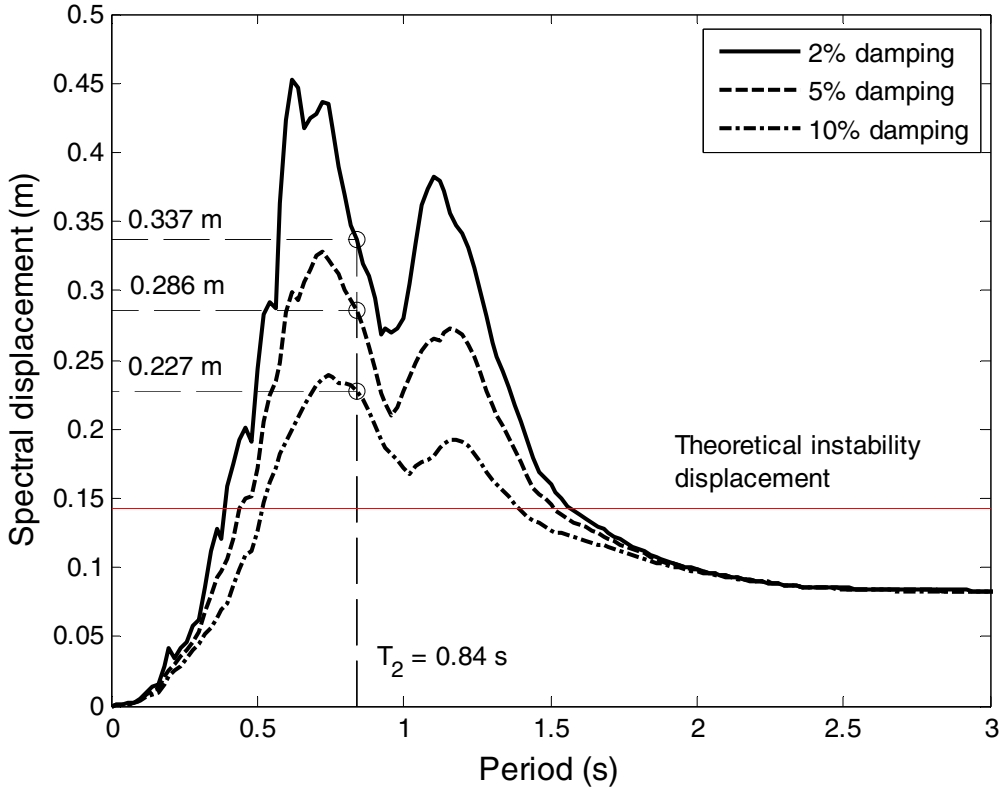

Figure 11: Displacement assessment of the stone building façade under the largest excitation

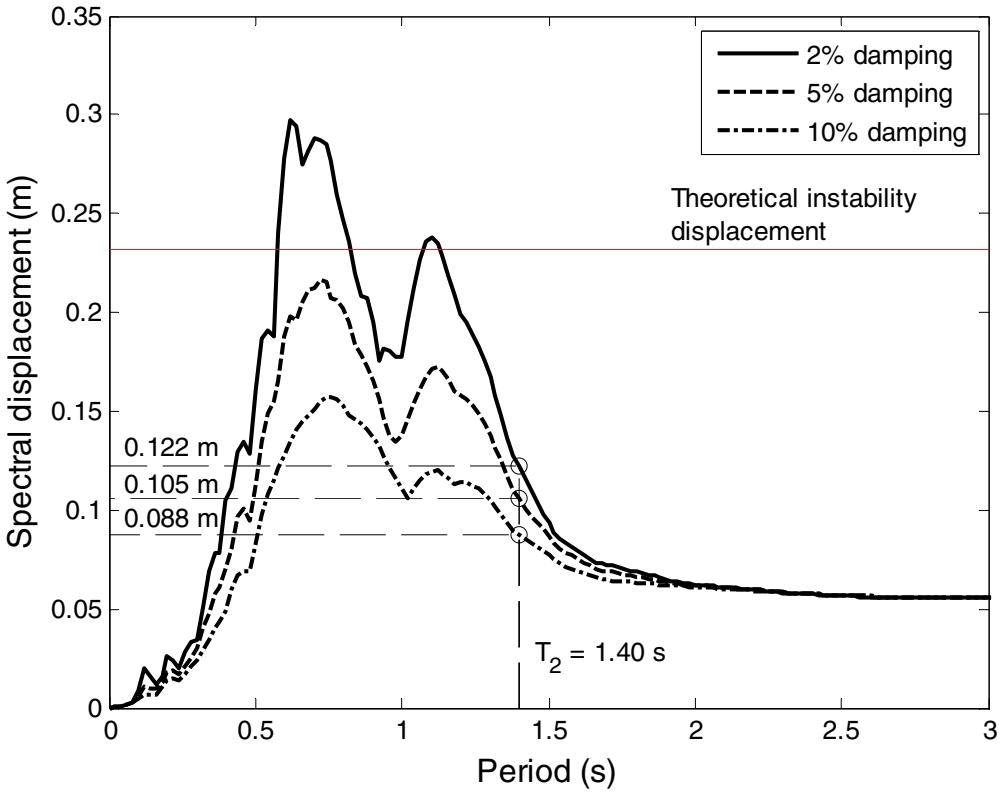

Table 1: Estimation of the substitute linear structure period

1	2	3	4	5	6	7
	M_{eff}, kg	$\Delta_{ins,\ eff}$, m	$\Delta_{t,ins}$, m	a_{ins}, g	$K_{2,\text{eff}}$, kN/m	T_2, sec
Brick	=0.64M=526	$0.560\Delta_{t,\text{ins}}$	1.09t=0.256	0.268	29.3	0.84
Stone	=0.81M=7264	$0.505\Delta_{t,\text{ins}}$	0.92t= 0.460	0.155	145.6	1.40

Table 2: Calculation of the wall maximum displacement using 5% damped response spectra

1	2	3	4	5	6
Test	Calculated displacement, mm		Measured Δ_t (mm)	Test observations	Comments
	Δ_{eff}	Δ_t			
Brick tests 1-5	50-143	90-256	0.1-0.9	No damage	Method overly conservative as the wall either did not crack or did not rock beyond Δ_2
Brick tests 6-7	191-236	340-420	2-6	Hairline cracking	
Brick test 8	286	510	>230 (collapse)	Collapse of facade	Collapse predicted
Stone test 1-3	38-54	75-106	1-3	No damage	Method overly conservative as the wall either did not crack or did not rock beyond Δ_2
Stone test 4-5	70-97	140-190	8-25	Slight rocking	
Stone final test 6	105	208	219	Near collapse	Correct prediction